9444–9455 Nucleic Acids Research, 2018, Vol. 46, No. 18 Published online 25 July 2018
doi: 10.1093/nar/gky656

Function of TFIIIC, RNA polymerase III initiation factor, in activation and repression of tRNA gene transcription

Małgorzata Cieśla, Ewa Skowronek and Magdalena Boguta*

Department of Genetics, Institute of Biochemistry and Biophysics, Polish Academy of Sciences, Pawińskiego 5A, 02-106 Warsaw, Poland

Received March 19, 2018; Revised July 09, 2018; Editorial Decision July 10, 2018; Accepted July 10, 2018

ABSTRACT

Transcription of transfer RNA genes by RNA polymerase III (Pol III) is controlled by general factors, TFIIIB and TFIIIC, and a negative regulator, Maf1. Here we report the interplay between TFIIIC and Maf1 in controlling Pol III activity upon the physiological switch of yeast from fermentation to respiration. TFIIIC directly competes with Pol III for chromatin occupancy as demonstrated by inversely correlated tDNA binding. The association of TFIIIC with tDNA was stronger under unfavorable respiratory conditions and in the presence of Maf1. Induction of tDNA transcription by glucose-activated protein kinase A (PKA) was correlated with the down-regulation of TFIIIC occupancy on tDNA. The conditions that activate the PKA signaling pathway promoted the binding of TFIIIB subunits, Brf1 and Bdp1, with tDNA, but decreased their interaction with TFIIIC. Association of Brf1 and Bdp1 with TFIIIC was much stronger under repressive conditions, potentially restricting TFIIIB recruitment to tDNA and preventing Pol III recruitment. Altogether, we propose a model in which, depending on growth conditions, TFIIIC promotes activation or repression of tDNA transcription.

INTRODUCTION

Transcription of nuclear genes in yeast and mammals is directed by three nuclear RNA polymerases. Polymerase III (Pol III) is dedicated for genes encoding small non-coding RNAs, mostly transfer RNA (tRNA) genes. Pol III initiation complexes, including transcription factor TFIIIB, have been recently reconstructed by electron microscopy. Structural analyses explained how TFIIIB, composed of the TFIIB-related factor Brf1, Bdp1 protein and TATA-box binding protein, recruits Pol III in the yeast system and how Pol III opens the promoter DNA (1,2).

Once formed, TFIIIB–DNA complexes are extremely stable; however, TFIIIB by itself is unable to bind to TATA-less promoters that are common to Pol III genes (3). Unlike Pol II, the Pol III machinery includes a specific initiation factor, TFIIIC, which recognizes and binds Pol III-specific promoter elements and subsequently recruits TFIIIB to the transcription start site (reviewed in (4,5)). Pol III promoter elements are commonly located within the transcribed regions. For all tRNA genes (except for the selenocysteine tRNA gene), these are internally located *cis*-acting control sequences called A- and B-boxes. At the tRNA level these elements constitute the universally conserved D- and T-loops, which in some tRNA genes (61 out of 274), are separated by an intron. Therefore, the distance between these two promoter elements can vary from 31 to 93 nt (reviewed in (6,7)). TFIIIC is a large six-subunit protein complex organized into two globular domains, τA and τB, which specifically recognize and bind A- and B-boxes, respectively. The main determinant of both, the selectivity and stability of TFIIIC–DNA complexes, is τB module binding to the B-box, whereas the A-box seems to be rather involved in transcription initiation (reviewed in (8)). Although tRNA genes vary significantly in length (from 72 to 133 nt), all remain fully covered by TFIIIC complexes, which exhibit remarkable structural elasticity (9).

Pol III is negatively regulated by the Maf1 protein, conserved from yeast to humans. Maf1 is not a typical DNA-binding transcription factor. Instead of binding to promoter elements, Maf1 binds directly the Pol III complex (10,11). Moreover, Pol III–Maf1 association is increased under unfavorable growth conditions and correlated with reduced Brf1 and Pol III occupancy at Pol III genes (12,13). Previous data suggested that Maf1 inhibits assembly of the TFIIIB–DNA complex and Pol III recruitment (14). The interplay between Maf1 and TFIIIC has not been addressed yet.

*To whom correspondence should be addressed. Tel: +48 22 592 1322; Fax: +48 22 592 2190; Email: magda@ibb.waw.pl
Present address: Ewa Skowronek, Laboratory of Bioinformatics and Protein Engineering, International Institute of Molecular and Cell Biology, Ks. Trojdena 4, 02-109 Warsaw, Poland.

The τB module of TFIIIC comprises of τ138 (Tfc3), τ91 (Tfc6) and τ60 (Tfc8) subunits, while τA is composed of τ131 (Tfc4), τ95 (Tfc1) and τ55 (Tfc7). This composition appears to be conserved, with homologs for each yeast subunit identified also in the human TFIIIC (15). Although only τ95 and τ138 bind DNA directly, all six subunits of TFIIIC are essential *in vivo*. The current model of TFIIIC architecture was provided based on structural information obtained from individual subunits and protein cross-linking data (16). The most important link between τA and τB modules is established by interaction of the disordered region of τ138, termed the τ-interacting region (τIR), with the tetratricopeptide domain (TPR) of τ131. This disordered region in τ138 provides the necessary flexibility for binding variously spaced A- and B-box promoters (16). In addition, the model of TFIIIC architecture provides insight into sites of TFIIIC interaction with TFIIIB and proposes a mechanism of TFIIIB recruitment (16).

According to early *in vitro* data, TFIIIC is only required for TFIIIB and Pol III recruitment and is displaced from DNA during Pol III transcription (referred in (5)). Other *in vitro* data suggest, however, that TFIIIC is not released from the DNA template once it is bound. In detail, preincubation of TFIIIC with one tRNA gene, followed by addition of a second template as a competitor exclusively led to the production of RNA corresponding to the first gene added (17). *In vivo* data show that TFIIIC is present at all transcriptionally active Pol III genes although its absolute binding efficiency is relatively low in comparison to TFIIIB and Pol III (18–20).

Another role of TFIIIC during ongoing transcription was further suggested by a recent genome-wide analysis of nascent transcripts attached to Pol III (21). Although tRNA genes are short, a strikingly uneven distribution of polymerases along transcription units was observed, suggesting regional deceleration of elongation or transient pausing of the polymerase. Inspection of individual tRNA genes showed a predominant pattern with a high density of nascent transcripts over the 5′ end and a weaker peak before the 3′ end of the gene. Interestingly, the 5′ and 3′ peaks of the transcribing Pol III coincide, respectively, with the beginning of the A-box and the B-box of the internal promoter. This suggested that TFIIIC bound to the A- and B-boxes could slow down the Pol III elongation rate leading to transient pausing events.

In addition, the function of TFIIIC may be controlled by signaling cascades since five subunits of TFIIIC (τ138, τ131, τ95, τ91 and τ55) were identified as phosphoproteins by global proteomic-based studies (22–24). Moreover, τ138, τ131 and τ95 were found to be phosphorylated *in vivo* (25), whereas τ91 and τ55 were phosphorylated *in vitro* (26). The significance of phosphorylation in the control of TFIIIC function has not been established yet.

In the present work, we report the results of chromatin immunoprecipitation (ChIP) studies aimed at elucidating the control of TFIIIC occupancy on tRNA encoding gene (tDNA) by environmental conditions. We show that alterations in occupancy of TFIIIC are inversely correlated with Pol III occupancy and depend on Maf1. Pol III activation is also correlated with an unexpected change in TFIIIC–TFIIIB interaction. Finally, we provide a model of how environmental conditions control TFIIIB recruitment by TFIIIC.

MATERIALS AND METHODS

Yeast strains and plasmids

Strains and plasmids used in this study are listed in Supplementary Tables S1 and S2. *Saccharomyces cerevisiae* strains are derivatives of BY4741 or YPH499.

Media and growth conditions

According to the 'YPD→YPGly' growth protocol, yeast cells were grown in medium containing 1% yeast extract, 2% peptone and 2% glucose (YPD) to the exponential phase and then transferred to YPGly medium (1% yeast extract, 2% peptone and 2% glycerol) and incubated at 37°C for 2 h. Based on the 'YPGly→YPGly+glucose' growth protocol, cells were grown in medium containing 1% yeast extract, 1% peptone, 3% glycerol and 0.1% glucose (YPGly) to the exponential phase, after which D-glucose was added to a final concentration of 100 mM (YPGly+glucose).

Chromatin immunoprecipitation (ChIP)

ChIP assay was performed as described previously with some modifications (27). Chromatin isolation and immunoprecipitation were done in lysis buffer (50 mM HEPES–KOH (pH 7.5), 150 mM NaCl, 1 mM ethylenediaminetetraacetic acid (EDTA), 1% Triton X-100, 0.1% Na-deoxycholate, 0.1% sodium dodecyl sulphate (SDS), O-complete protease inhibitor; Roche). Exceptionally for τ138-TAP ChIP, modified lysis buffer (0.02% Na-deoxycholate, 0.02% SDS, 50 mM HEPES–KOH (pH 7.5), 150 mM NaCl, 1 mM EDTA, 1% Triton X-100, O-complete protease inhibitor) was used. For ChIP assays, chromatin was incubated with mouse or rabbit Dynabeads IgG magnetic beads (Invitrogen) and the following mouse antibodies: anti-HA (Covance) (3 μg for C160-HA and Bdp1-HA ChIP), anti-green fluorescent protein (GFP) (Roche) (2 μg for τ131-GFP ChIP and negative control for Bdp1-HA ChIP), anti-Myc (Roche) (2 μg, negative control for C160-HA ChIP and for τ131-GFP ChIP) or the following rabbit antibodies: anti-τ138 (Gramsh) (3 μg for τ138-TAP ChIP), anti-Brf1 (Gramsh) (3 μg for Brf1 ChIP) or control rabbit pre-immune serum IgG (GenScript) (3 μg for τ138-TAP ChIP and for Brf1 ChIP). Beads with bound chromatin were washed one time in lysis buffer and three times in high-salt lysis buffer (500 mM NaCl), except for τ138-TAP ChIP in case of which beads were washed one time in modified lysis buffer and two times in modified high-salt lysis buffer (500 mM NaCl). Then, beads were washed one time in the immunoprecipitation (IP) buffer (10 mM Tris (pH 8), 280 mM LiCl, 1 mM EDTA, 0.5% Na-deoxycholate and 0.5% tergitol (NP-40)). Elution from beads, de-crosslinking and DNA purification were done as described previously (28).

Quantitative PCR

qPCR of immunoprecipitated DNA fragments was performed in 384-well plates using the Roche LightCycler 480

machine. PCR reactions (10 μl volume) contained 2 μl of DNA template, 300 nM primer pairs and 5 μl of RT PCR Mix SYBR (A&A Biotechnology). Primer sequences are given in Supplementary Table S3. All reactions were conducted in triplicate and each set included a no template control. The amplification reaction consisted of 5-min of preincubation in 95°C and 45 cycles of amplification at 95°C for 15 s, 55°C for 20 s and 72°C for 20 s. A melting curve analysis was performed for each sample after PCR amplification to ensure that a single product with the expected melting curve characteristics was obtained. Each experimental set comprised of a standard curve, established with PCRs of serial dilutions of the input DNA. Data were processed in Roche LightCycler software release 1.5.0 and then analyzed in Excel (Microsoft). Occupancy values were calculated by determining the immunoprecipitation efficiency that is the amount of PCR product in the immunoprecipitated sample divided by the amount of PCR product in the input sample multiplied by 100. All the values of tDNA occupancy by proteins of Pol III machinery together with the respective controls and standard error of the mean (SEM) are listed in Supplementary Tables S5–S13.

Northern analysis

RNA isolation and Northern hybridization was done as described previously (29), using 3 or 5 μg of RNA separated by electrophoresis on 10% polyacrylamide, 8 M urea gel. Digoxigenin-UTP (DIG) -labeled oligonucleotides used for RNA hybridization are described in Supplementary Table S4.

Western analysis

Total protein extracts and immunoprecipitated proteins were separated by 6% or 8% sodium dodecyl sulphate-polyacrylamide gel electrophoresis (SDS-PAGE) and hybridized with mouse monoclonal antibodies anti-HA (Covance) at a 1:5000 dilution for 2 h, anti-GFP (Roche) at a 1:5000 dilution for 1 h, anti-Pgk1 (Invitrogen) at a 1:20 000 dilution for 0.5 h and with rabbit polyclonal antibodies against Brf1 (Gramsh) at a 1:1000 dilution for 2 h or peroxidase anti-peroxidase (PAP) antibody (Sigma-Aldrich) at a 1:5000 dilution for 1 h. Then, nitrocellulose membranes were incubated with secondary anti-mouse or anti-rabbit antibodies coupled to horseradish peroxidase (Dako) at a dilution of 1:5000 for 1 h and visualized by chemiluminescence using the ECL detection kit (Bio-Rad).

τ138–τ131 co-immunoprecipitation

Extracts were prepared in IP buffer (50 mM HEPES–KOH, pH 7.5, 100 mM NaCl, 1 mM EDTA, 0.05% NP-40, 0.5 mM ditiotreitol (DTT), 5% glycerol, O-complete protease inhibitor; Roche) by mechanical disruption with beads as described before (30). Mouse Dynabeads IgG magnetic beads (50 μl) (Invitrogen), washed three times with 0.5% bovine serum albumin (BSA) in phosphate-buffered saline (PBS), were incubated overnight with equal amounts (0.5 mg) of protein extracts in IP buffer with gentle shaking at 4°C. Immunoprecipitation of τ138-TAP together with bound proteins is based on the affinity of immunoglobulin G (IgG) to the protein A-containing TAP tag. After incubation, beads were washed two times with IP buffer and two times in high-salt IP buffer (450 mM NaCl). Immunoprecipitated proteins were eluted by boiling for 5 min in SDS sample buffer and analyzed on 6% SDS-PAGE gel by western blotting with PAP and anti-GFP antibodies.

τ138–Bdp1 and τ138–Brf1 co-immunoprecipitation

Cells were cross-linked with 1% formaldehyde for 30 min at room temperature, washed twice in PBS and pelleted. Extracts were prepared in ChIP lysis buffer as described previously (13). Mouse Dynabeads IgG magnetic beads (50 μl) (Invitrogen), washed three times with 0.5% BSA in PBS, were incubated with mouse anti-HA antibody (3 μg) or mouse anti-GFP antibody (2 μg) for 3 h at 4°C. After extensive washing in PBS containing 0.5% BSA and then in IP buffer, beads were incubated with 1.5 mg of protein extracts in ChIP buffer for 4 h with gentle shaking at 4°C. For τ138-GFP immunoprecipitation, beads were washed four times with ChIP lysis buffer (250 mM NaCl). For Bdp1-HA immunoprecipitation, beads were washed three times with ChIP lysis buffer (250 mM NaCl) and one time with ChIP lysis buffer (350 mM NaCl). For DNase treatment, beads after immunoprecipitation were washed once with ChIP and once with DNase buffer (25 mM $MgCl_2$, 10 mM $CaCl_2$, 10 mM Tris–HCl (pH 7.5) 25 mM NaCl). Then half of the beads were incubated with 25U of DNase (Thermo Scientific) for 30 min at 37°C and washed (3×) with ChIP lysis buffer containing 250 mM NaCl. Elimination of DNA from the extracts was monitored by PCR with selective primers for tRNA genes (Supplementary Table S3). Samples were eluted directly into the SDS sample buffer by incubation for 15 min at 90°C before running on 8% SDS-PAGE. Mouse anti-HA, mouse anti-GFP or rabbit anti-Brf1 antibodies were applied for detection using western blot technique.

RESULTS

Switch between fermentation and aerobic respiration causes opposite Maf1-dependent changes in Pol III and TFIIIC occupancy on tRNA genes

Variations in glucose availability in the natural environment force yeast to undergo frequent metabolic transitions between fermentation and aerobic respiration by using non-fermentable carbon sources. This switch causes widespread changes in gene transcription, including repression of tDNA transcription by Maf1 (31). Similarly to rapamycin stress, respiratory growth led to dephosphorylation and activation of Maf1 (31). In the dephosphorylated form, Maf1 binds directly to the Pol III complex that is correlated with Maf1-dependent dissociation of Pol III and TFIIIB from the chromatin (12).

Here, we have focused our study on the regulation of TFIIIC association with tRNA genes by the metabolic switch.

We investigated whether recruitment of TFIIIC to representative intron-containing and intron-less tRNA genes is dependent on Maf1 and how it is correlated with Pol III recruitment. Wild-type and *maf1*Δ mutant strains were grown in glucose medium under optimal conditions (YPD) and then transferred and incubated in medium containing glycerol (YPGly), a non-fermentable carbon source, at 37°C for 2 h. This growth protocol, referred further as 'YPD→YPGly', leads to a metabolic switch that activates Maf1 (31). Both wild-type and *maf1*Δ harbored one epitope-tagged bait, namely TAP-tagged τ138, the largest subunit of TFIIIC that interacts directly with B-boxes in tDNA or HA-tagged C160, the largest catalytic subunit of Pol III.

The efficiency of TAP-tagged τ138 immunopurification was greatly increased by using a τ138-specific antibody (Supplementary Figure S1). Enrichment of tDNA fragments immunopurified with antibodies directed to epitope tags was estimated by quantitative polymerase chain reaction (qPCR) with primers that span transcribing regions. Occupancy of τ138 on selected tRNA genes has been shown as a percentage of immunoprecipitation over input chromatin (Figure 1A). tDNA occupation by τ138 during active transcription in wild-type YPD cells increased upon YPD→YPGly transition, especially for intron-containing tDNA-Leu and tDNA-Phe. Clearly, the dynamics of TFIIIC occupancy was affected by *maf1*Δ, although the effect was limited to intron-containing genes. While in the wild-type strain YPD→YPGly transition resulted in about a 2.5-fold increase of τ138 occupancy on tDNA-Leu and tDNA-Phe, the increase observed for the *maf1*Δ mutant was ∼1.5-fold. These differences are statistically significant (Figure 1A). Variations of τ138 occupancy on intron-less tDNA-Val and tDNA-Met genes were less pronounced, and the effects of *maf1*Δ were not statistically significant. Altogether, the switch between fermentation and aerobic respiration increases TFIIIC occupancy on intron-containing tRNA genes in a Maf1-dependent manner. This observation is consistent with our previous finding that tRNAs encoded by intron-less genes are less sensitive to Maf1-mediated regulation (31,32).

The Pol III ChIP showed a strong effect of *maf1*Δ on the occupancy of C160 on both intron-containing and intron-less tRNA genes (Figure 1B), which is consistent with previous data (12) and accurately reflects the observed transcriptional changes (Figure 1C and D). In the wild-type strain, substantial decrease of Pol III association with tRNA genes and transcription of pre-tRNA was observed upon YPD→YPGly transition. In contrast, no decrease but even modest increase of Pol III occupancy on tDNAs was seen in the *maf1*Δ mutant, which correlated with accumulation of primary transcripts and intron-containing tRNA precursors (Figure 1 A and D).

In summary, we conclude that the YPD→YPGly transition causes opposite changes in Pol III and TFIIIC occupancy on tRNA genes. Regulation of tDNA transcription by the metabolic switch is dependent on Maf1 and is consistent with the regulation of Pol III occupancy. Importantly, opposite regulation of TFIIIC occupancy, especially on intron-containing genes, is also dependent on Maf1.

Glucose-induced Pol III transcription mediated by PKA signaling correlates with Maf1-dependent release of TFIIIC from tRNA genes

Major changes in gene expression are observed in yeast when glucose becomes available for cells grown in a non-fermentable carbon source. This response is mainly dependent on glucose activation of the central signaling pathway, protein kinase A (PKA). In general, the PKA pathway stimulates transcription of genes promoting translation and growth (33). Here, we examined induction of tDNA transcription under conditions corresponding to PKA activation (34). Cells were grown in glycerol medium to the exponential phase, and subsequently glucose was added to a final concentration of 100 mM, followed by a 15 min incubation (the growth protocol is referred further as YPGly→YPGly+glucose). Primary transcripts of tRNA-Leu were undetectable in YPGly cells harvested in the logarithmic phase but appeared within 5 min after the addition of glucose, indicating rapid activation of tRNA synthesis (Figure 2A, left panel). This activation was, however, attenuated in double *tpk1*Δ *tpk2*Δ mutant with inactive catalytic PKA subunits (Figure 2A and B). Thus, PKA appears to be important for Pol III activation upon YPGly→YPGly+glucose transition of yeast. Furthermore, PKA was previously found to prevent Pol III repression by Maf1 (35).

Subsequent ChIP analyses of tRNA gene occupancy by the Pol III machinery also revealed opposite effects on TFIIIC and Pol III, a decrease in τ138 recruitment and an increase in C160 recruitment and upon YPGly→YPGly+glucose transition when PKA becomes fully active (34). In short, association of both TFIIIC and Pol III with chromatin is inversely controlled by glucose stimulation, which is correlated with the induction of PKA signaling. Moreover, this control is dependent on the presence of Maf1. In YPGly cells, recruitment of C160 to tRNA genes was much higher in *maf1*Δ mutant than control wild-type strain, and further increases when glucose was supplied (Figure 2D). In contrast, in YPGly cultures, recruitment of τ138 to tRNA genes in *maf1*Δ mutant was relatively lower than in control strain (Figure 2C). Moreover, addition of glucose resulted in an even greater decrease of τ138 occupancy (Figure 2C). Thus, we concluded that Maf1 affects glucose-controlled occupancy of chromatin by TFIIIC and Pol III in an opposite manner.

Inactivation of potential sites of phosphorylation by PKA in τ138 subunit of TFIIIC prevents induction of tDNA transcription by glucose and strengthens interaction between τA and τB modules

We considered the possibility that phosphorylation by PKA could affect other Pol III associated proteins besides Maf1. Global proteomics-based screening for phosphorylated polypeptides in yeast identified τ138, indicating three serine residues (S104, S222 and S892) as potentially phosphorylation targets by the catalytic subunits Tpk1/Tpk3 of PKA (23). τ138 was also found to be phosphorylated *in vivo* (25). Together, these findings led us to explore the role of τ138 phosphorylation in control of tRNA synthesis.

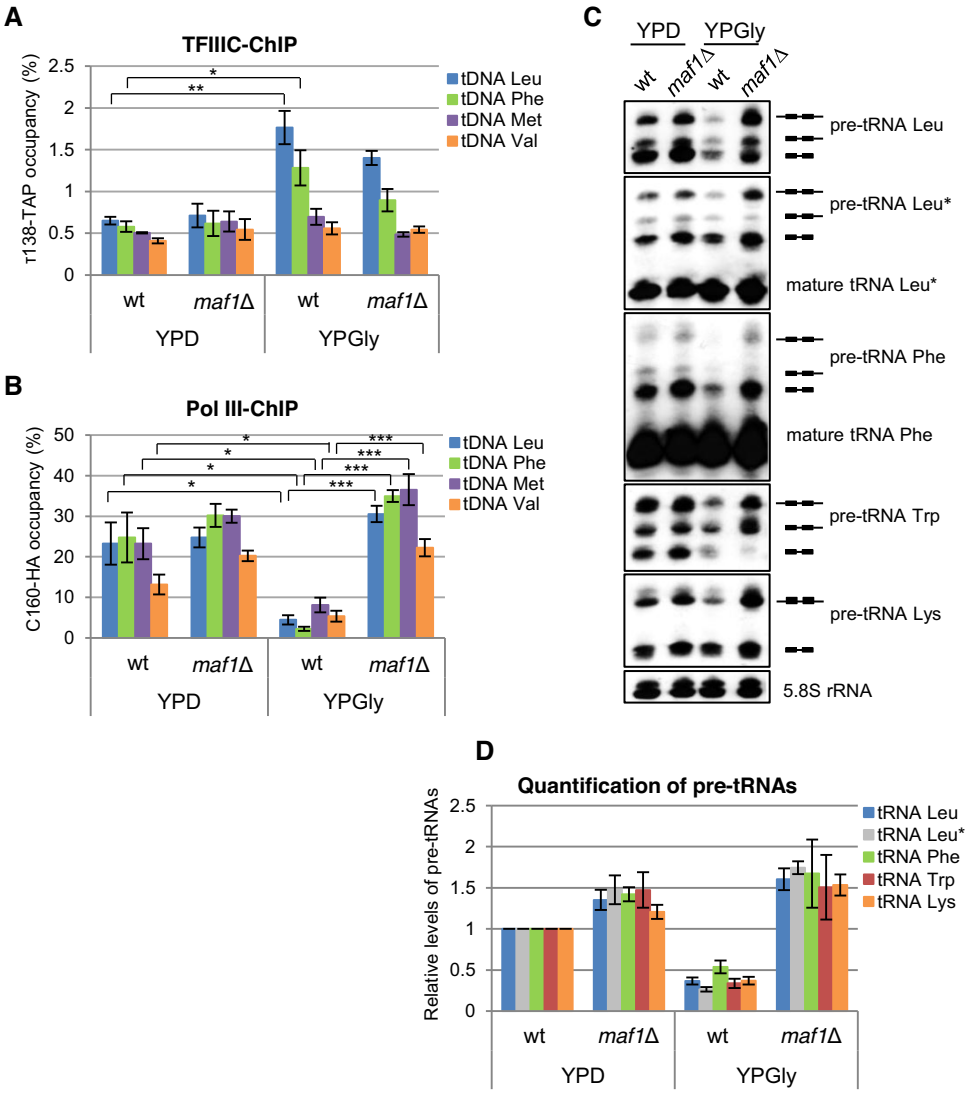

Figure 1. Switch between fermentation and aerobic respiration results in Maf1-dependent, inverse changes in Pol III and TFIIIC occupancy on tRNA genes. Control strain (wt) and isogenic *maf1*Δ mutant grown in glucose medium were harvested in the exponential phase (YPD) or transferred to glycerol medium and cultivated in YPGly for 2 h at 37°C (YPD→YPGly protocol). Cross-linked chromatin isolated from wt and *maf1*Δ strains expressing τ138 with TAP epitope (**A**) or C160 with HA epitope (**B**) was immunoprecipitated with antibodies against τ138 (A) or HA (B) followed by quantitative real-time PCR with primers specific for the following single tDNAs: intron containing tL(CAA)G1 and tF(GAA)H1 (designated as tDNA-Leu and tDNA-Phe) and intron-less tM(CAU)E and tV(CAC)D (designated as tDNA-Met and tDNA-Val, respectively). The occupancy is represented as a percentage of immunoprecipitation over input chromatin. See that scale is different in panels (A) and (B). (**C**) RNA isolated from wt and *maf1*Δ strains was analyzed by northern blotting using probes specific for given families of isoacceptor tRNAs: tRNA-Leu(CAA), tRNA-Leu(UAG) [designated tRNA-Leu*], tRNA-Phe(GAA), tRNA-Trp(CCA) and tRNA-Lys(UUU). Some probes detect only intron-containing tRNA precursors, primary transcripts (designated ▬▬) and 5′- or 5′,3′-end-matured forms (designated ▬▬ or ▬▬, respectively), whereas other probes also recognize mature tRNA. 5.8S rRNA served as a loading control. (**D**) Amounts of primary transcripts (▬▬) were normalized to the loading control and calculated relative to amounts in the wt strain under standard conditions (YPD), which was assumed as 1. Bars in panels (A), (B) and (D) represent the mean ± standard error of the mean (SEM) of three independent experiments. *p* values were calculated using a two-tailed t-test. ***, ** and * asterisks indicate, respectively, *p* value <0.005, <0.01 and <0.05.

Although we were unable to detect changes in growth and phosphorylation patterns on gels, *de novo* synthesis of tRNA-Phe was attenuated in τ138–*3StA* (S104A, S222A and S892A) strains (Figure 3A); however, the statistically significant difference in transcription was detected only when cells were harvested 10 and 15 min after glucose addition (Figure 3B). Notably, the observed transcription inhibition was related to the created mutations as they were complemented by the native *TFC3* gene introduced on a plasmid (Supplementary Figure S2). Therefore, the contribution of PKA phosphorylation sites may be important for τ138 function.

Next, we investigated whether the τ138–*3StA* mutation affected recruitment of mutant TFIIIC to tDNA. When the YPGly→YPGly+glucose growth protocol was applied for wild-type and τ138–*3StA* mutant, ChIP inspections showed the difference between wild-type and τ138–*3StA* mutant on YPGly cells, but not 10 min after addition of glucose (YPGly+glucose) when transcription was activated (Figure 3C). ChIP experiment was repeated in the *tpk1*Δ

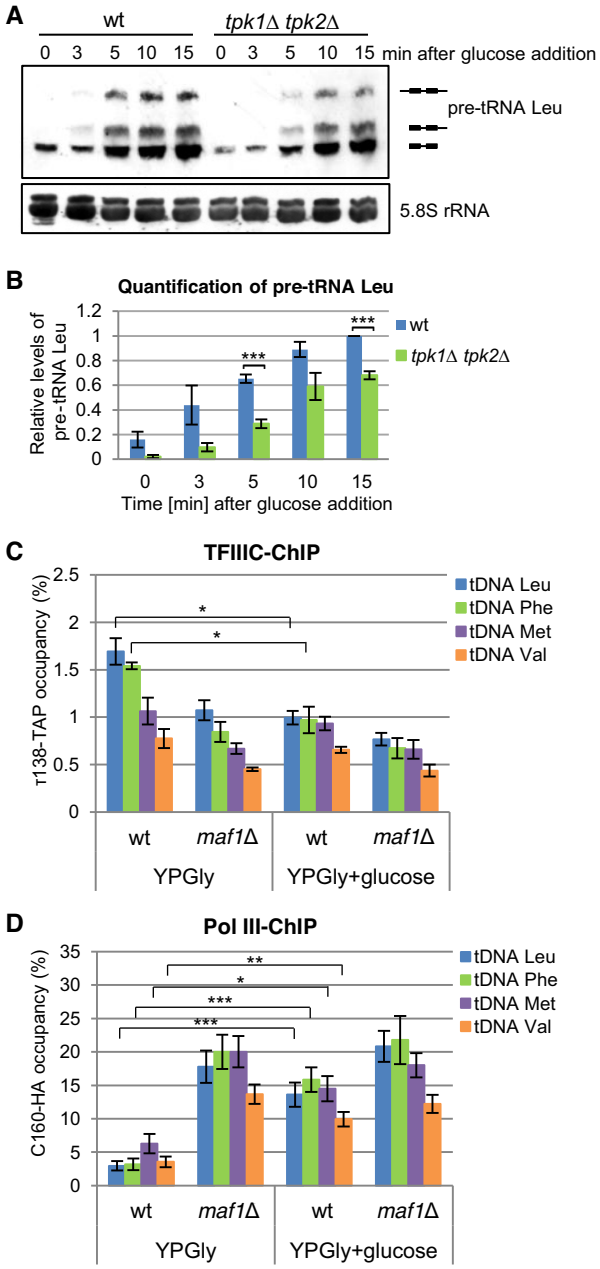

Figure 2. Addition of glucose to yeast cultivated in medium with a non-fermentable carbon source results in rapid induction of tDNA transcription and opposite, Maf1-dependent, changes in Pol III and TFIIIC recruitment to tDNA. Yeast were grown in glycerol medium at 30°C (YPGly) to the logarithmic phase, then glucose was added to a final concentration of 100 mM (YPGly+glucose) and samples were taken at desired times (YPGly→YPGly+glucose protocol). Northern blot analysis (A) and quantification of primary transcript for tRNA-Leu(CAA) (B) in control (wt) and isogenic mutant strains with inactive PKA kinase (*tpk1*Δ *tpk2*Δ). Amounts of primary transcripts (▬▬) normalized to loading control and calculated relative to amount in control wt strain, 15 min after glucose addition that was assumed as 1. Probe specific for tRNA-Leu(CAA) detects primary transcript (designated ▬▬) and 5′- or 5′,3′-end-matured pre-tRNA (designated ▬▬ or ▬▬). 5.8S rRNA served as a loading control. Occupancy of tDNAs by TFIIIC (C) and Pol III (D). Cross-linked chromatin isolated from wt and *maf1*Δ strains expressing the τ138-TAP (C) or C160-HA epitope fusion (D) was immunoprecipitated and analyzed as described in the legend to Figure 1. Samples were taken 10 min after glucose addition. ***, ** and * asterisks indicate, respectively, *p* value <0.005, <0.01 and <0.05.

*tpk2*Δ PKA knockout strain (Supplementary Figure S3). The comparable effects of *tpk1*Δ *tpk2*Δ and τ138–*3StA* mutants on τ138 association with tDNA suggest that PKA may control the TFIIIC occupancy on Pol III chromatin.

Recruitment of τ131, another subunit of TFIIIC, to tRNA genes was also moderately affected by τ138–*3StA* mutation (Figure 3D), in contrast to the pure effect on tDNA transcription (Figure 3A and B). Thus, we considered another possible function of τ138, which is strongly affected by the τ138–*3StA* mutation.

The model of TFIIIC architecture implicated the τIR domain of τ138 as a crucial component for linking τA and τB modules. The docking platform for τIR is provided by the N-terminal part of the τ131 subunit of τA (16). To investigate the possible effect of τ138–*3StA* on the interaction of mutant τ138 with τ131, yeast cells expressing TAP-tagged wild-type or mutated τ138 and GFP-tagged τ131 were grown according to YPGly→YPGly+glucose protocol and examined by co-immunoprecipitation. τ138 was immunopurified from crude extracts and analyzed by western blot (Figure 3E). The levels of τ131 co-precipitated with wild-type τ138 were unchanged when glucose was added inducing DNA transcription. In contrast, glucose addition to τ138–*3StA* cells resulted in a significant increase in τ131 levels bound to τ138–*3StA* (Figure 3E). Thus, we concluded that inefficient induction of tDNA transcription by glucose in τ138–*3StA* cells correlated with a stronger interaction between mutated τ138 and τ131. It seems possible that phosphosite mutations trigger increased binding of mutated τ138 to τ131 and affect the flexibility of the TFIIIC complex, which is ultimately necessary to accomplish induction of tDNA transcription via the PKA pathway.

Increased interaction of τ131 subunit of TFIIIC with Bdp1 and Brf1 subunits of TFIIIB during transcription repression

Very important role of TFIIIC in the regulation of transcription by Pol III is the assembly of TFIIIB upstream of the transcription start site. The mechanism by which TFIIIC recruits TFIIIB onto tRNA genes appears to involve a stepwise series of intricate protein–protein and protein–DNA interactions, the details of which are poorly understood. One of the crucial steps in TFIIIB assembly is the interaction between τ131 and the Bdp1 subunit of TFIIIB (36,37). Moreover, the current hypothesis suggests a competition between Bdp1 and τ138 for interaction with the same τ131 domain (16).

To examine connections between growth conditions and TFIIIB assembly by TFIIIC, we determined whether induction of Pol III activity equally affected the direct interaction between τ131 and TFIIIB subunits, Bdp1 and Brf1, and their recruitment to tRNA genes. At the same time, we also examined TFIIIB assembly in τ138–*3StA* mutant. Considering the current model (16), the increased interaction of τ131 with τ138–*3StA* (Figure 3E) should somehow affect association of τ131 with Bdp1. We took advantage of the result that Pol III activity was rapidly induced upon YPGly→YPGly+glucose transition. That growth protocol was employed for wild-type and τ138–*3StA* mutant strains expressing either GFP-tagged τ131 or HA-tagged Bdp1 or both. YPGly cells harvested in the logarithmic phase or

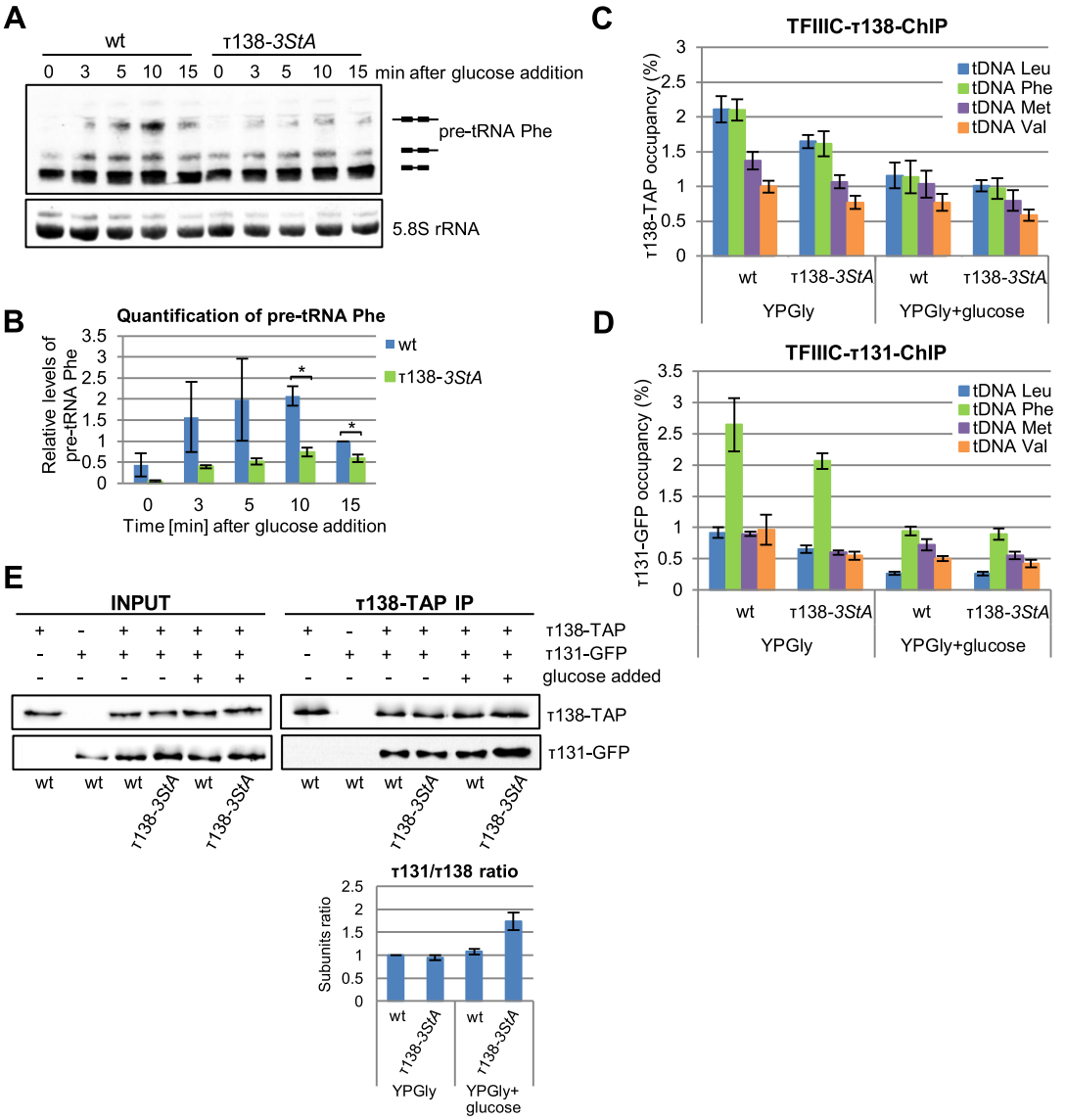

Figure 3. Multiple consequences of the inactivation of potential sites of phosphorylation by PKA in τ138 subunit of TFIIIC. τ138–*3StA* mutant and corresponding wild-type strains were grown according to YPGly→YPGly+glucose protocol. Samples were taken at desired times after glucose addition. Experiments were performed in triplicate to calculate SEM represented by error bars. (**A** and **B**) Attenuation of tRNA transcription. Northern blot analysis (A) and quantification of primary transcript for tRNA-Phe(GAA) (B). Amounts of primary transcripts (▬▬) normalized to loading control and calculated relative to amount in control wt strain, 15 min after glucose addition that was assumed as 1. * asterisk indicates p value <0.05. (**C** and **D**) Recruitment of TFIIIC to tDNAs. Occupancy of tDNAs by τ138 (C) and τ131 (D). Cross-linked chromatin isolated from wt and τ138–*3StA* strains expressing τ138-TAP epitope (C) or τ131-GFP epitope (D) was immunoprecipitated and analyzed as described in the legend to Figure 1. Samples were taken 10 min after glucose addition. (**E**) Inactivation of potential sites of phosphorylation by PKA in τ138 strengthens the interaction between τA and τB modules of TFIIIC. Total cellular extracts (INPUT) prepared from wt and τ138–*3StA* mutant strains expressing GFP-tagged τ131 and TAP-tagged τ138 or τ138–*3StA* and from control strains expressing only a τ131-GFP or τ138-TAP tag were subjected to immunoprecipitation using IgG-coated magnetic beads. This protocol is based on the affinity of the protein A-containing TAP tag to IgG. Immunoprecipitated proteins were eluted and analyzed by sodium dodecyl sulfate-polyacrylamide gel electrophoresis (SDS-PAGE) and western blot using peroxidase anti-peroxidase (PAP) and anti-GFP antibodies. Band intensities from western blot images were quantified by MultiGauge v3.0 software (Fujifilm). τ131/τ138 ratios were calculated, and the τ131/τ138 ratio in wt strains grown in YPGly medium was set to 1.

10 min after glucose addition (YPGly+glucose) were tested in parallel for the τ131–Bdp1 and τ131–Brf1 interactions by co-immunoprecipitation (Figure 4A) and recruitment of Bdp1 and Brf1 to tDNA by ChIP (Figure 4B and C). To faithfully establish an assembly–recruitment relationship, we tested the TFIIIC–TFIIIB interaction in cross-linked chromatin. Immunoprecipitation of τ131 with magnetic beads coated with anti-GFP antibodies and further examination by western blotting revealed that the levels of co-purified Bdp1 and Brf1 were unaffected by τ138–*3StA* mutation but varied depending on the carbon source in the medium (Figure 4A, right panel). In YPGly cells, the levels of co-immunoprecipitated Bdp1 were ∼8-fold higher than YPGly+glucose cells. Treatment of immunoprecipi-

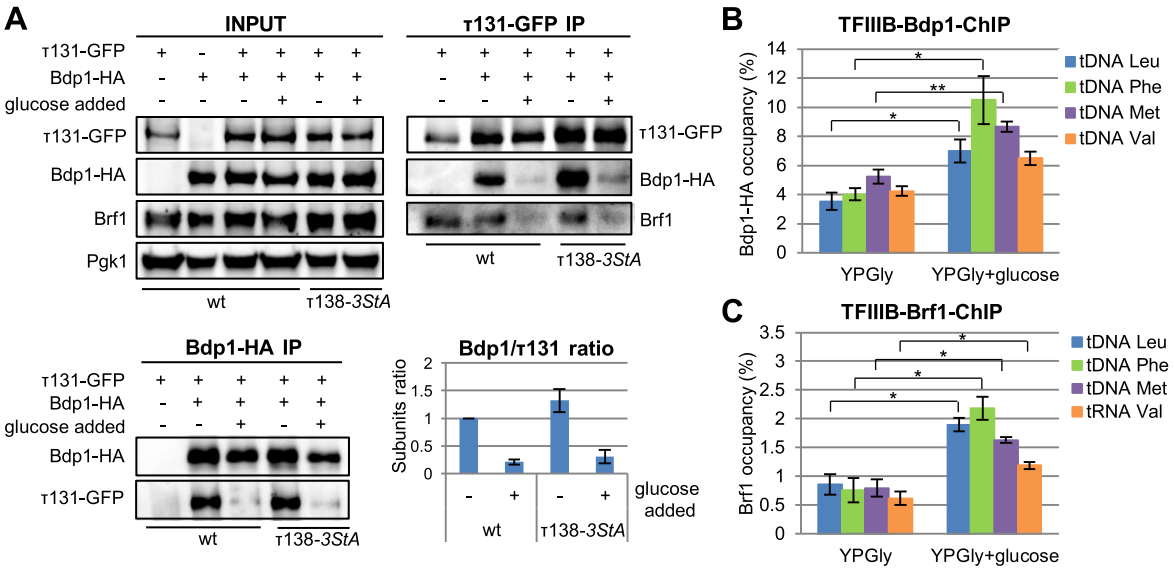

Figure 4. Assembly–recruitment relationships between TFIIIC and TFIIIB. τ138–*3StA* mutant and corresponding wild-type strains were grown according to YPGly→YPGly+glucose protocol. All experiments were performed in triplicate. (**A**) Increased TFIIIC–TFIIIB interaction during transcription repression. Cross-linked chromatin extracts isolated from wild-type and τ138–*3StA* mutant strains expressing double GFP-tagged τ131 and HA-tagged Bdp1 and controls expressing single-tagged τ131-GFP were subjected to immunoprecipitation with 1* magnetic beads coated with an anti-GFP antibody (right upper panel) or 2* magnetic beads coated with an anti-HA antibody (left lower panel), followed by elution of bound proteins. Immunopurified proteins were analyzed by SDS-PAGE and western blot using anti-HA, anti-GFP and anti-Brf1 antibodies. Band intensities from western blot images were quantified by MultiGauge v3.0 software (Fujifilm). Bdp1/τ131 ratios were calculated, and the ratio in wt strains grown in YPGly medium was set to 1. Differences between wt and τ138–*3StA* mutant were not statistically significant. (**B** and **C**) Increased TFIIIB occupancy on tDNA genes during transcription activation. Cross-linked chromatin isolated from wild-type and τ138–*3StA* mutant strains expressing HA-tagged Bdp1 was immunoprecipitated with antibodies against HA (B) or Brf1 (C), followed by qPCR as described in the legend to Figure 1.* and ** asterisks indicate, respectively, *p* value <0.01 and <0.05.

tates with DNase did not affect the binding of τ138 with Bdp1 and Brf1, excluding the possibility that their interactions are mediated by DNA (Supplementary Figure S3).

Moreover, reciprocal precipitation of Bdp1-HA co-precipitated τ131 more efficiently from extracts derived from YPGly cells (Figure 4A, left panel). Therefore, we concluded that the τ131–Bdp1 interaction is strong under repression conditions and drops when transcription is activated. Interestingly, ChIP analysis of TFIIIB recruitment to tRNA genes showed the opposite; relatively low Bdp1 occupancy YPGly cells was significantly increased after glucose was added (Figure 4B). Occupancy analyses of Brf1, resulted in a similar ∼2-fold increase in recruitment (Figure 4C). It is possible that Brf1 and Bdp1 assemble on TFIIIC during repression and are separated from tRNA genes until transcription is induced. Due to conformational change in τA module of TFIIIC, Brf1 and Bdp1 are specifically directed to the upstream transcription start site where they form a stable complex together with the independently delivered TATA-biding protein (TBP).

DISCUSSION

In the present work, we show the dynamics of TFIIIC association with tRNA genes during transition of yeast between fermentation and respiration. TFIIIC–Pol III associations with tRNA genes are inversely correlated and dependent on Maf1. Transitions between fermentation and respiration also affected TFIIIC-directed recruitment of TFIIIB. The TFIIIC–TFIIIB interaction in cross-linked chromatin was strong under respiratory conditions, whereas glucose promotes release of TFIIIB from TFIIIC and recruitment of TFIIIB to tRNA genes.

Examination of tDNA occupancy by TFIIIC and Pol III during metabolic transitions between fermentation and aerobic respiration (YPD→YPGly) and vice versa (YPGly→YPGly+glucose) confirmed previous notions that TFIIIC does not dissociate from chromatin during active transcription, but even throughout dynamically changing growth conditions remain more or less tightly associated with tDNA (18). Although ChIP experiments using different baits and antibodies cannot be directly compared quantitatively, we noticed an obvious inverse correlation between carbon source-dependent changes in TFIIIC and Pol III occupancy of tDNA. The YPD→YPGly transition of control wild-type strain resulted in a decrease in Pol III occupancy and increase in TFIIIC occupancy, whereas the YPGly→YPGly+glucose transition resulted in the opposite (Figure 5, upper panel). These opposite alterations suggest exclusivity between TFIIIC and Pol III.

Our results are in line with a previously reported genome-wide decrease in Pol III occupancy upon repression (in stationary phase, by nutrient starvation or rapamycin treatment) accompanied by an increase in TFIIIC occupancy (12,18,38). Moreover, glucose addition to nutrient-starved cells led to a reversal of this effect; TFIIIC was released from active genes, with the notion that transcription by Pol III partially displaces TFIIIC from its binding sites (18). Opposite changes in recruitment of Pol III and TFIIIC upon star-

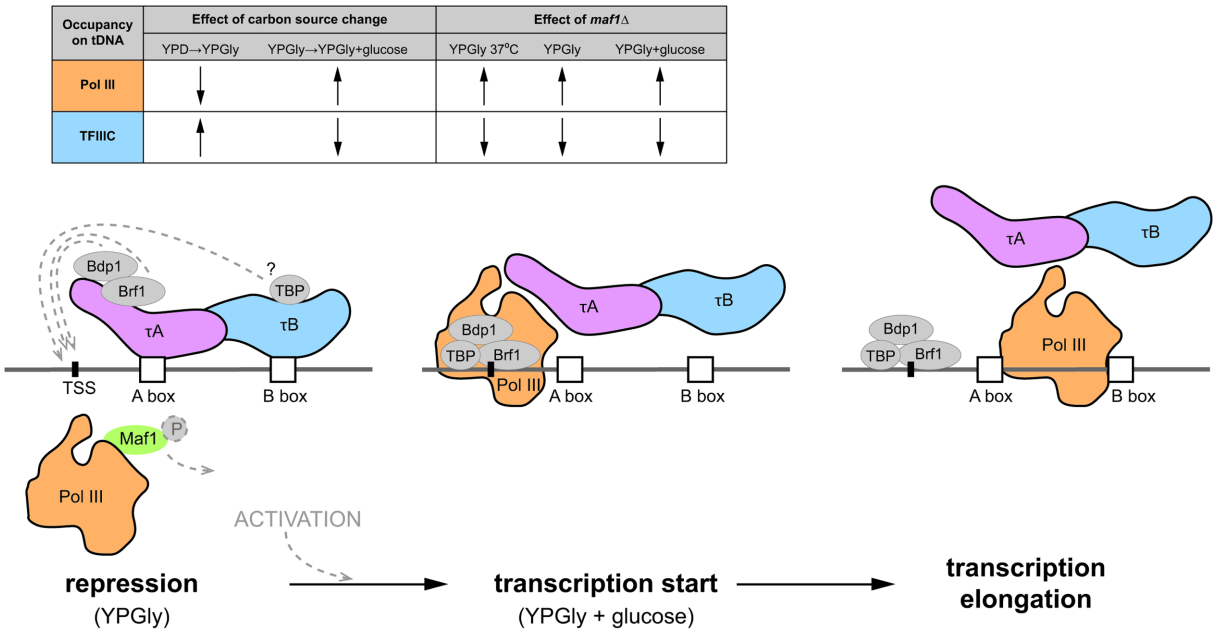

Figure 5. Competition between TFIIIC and Pol III for tDNA (upper panel). Inverse correlation between carbon source-dependent changes of Pol III and TFIIIC occupancies on tRNA genes in the wild-type strain and reverse changes of Pol III and TFIIIC occupancies in *maf1Δ* mutant—compared to wild-type strain—is shown by arrows indicating up- or down-regulation that could not be quantitatively compared. Molecular mechanism of TFIIIC-mediated recruitment of TFIIIB and control of tDNA transcription by Pol III (lower panel). During repression, TFIIIC associated with tDNA. Two subunits of TFIIIB, Brf1 and Bdp1, are bound to the τA module of TFIIIC. Pol III in complex with Maf1 is inactive. Transcription initiation, induced by environmental signal, leads to stepwise dissociation of TFIIIC from tDNA, correlated with the release of Brf1 and Bdp1 from the complex with τA and their subsequent transfer to tDNA. Formation of TFIIIB complex on tDNA possibly involves rearrangement of TBP, pre-bound to the τ60 subunit, which has been not studied here and is designated by a question mark. Recruitment of Pol III to the transcription start site is preceded by phosphorylation of Maf1 and its dissociation. Subsequent conformational changes in Pol III machinery lead to formation of an elongation complex and displacement of TFIIIC from tDNA by the transcribing polymerase. Presented protein–protein and protein–DNA interactions lead to stepwise DNA rearrangements, DNA bending, formation of a closed pre-initiation complex and promoter opening, which were beyond our study and are not shown.

vation were also demonstrated by ChIP only for the longest Pol III gene, *SCR1* (13).

Here, we examined changes of TFIIIC occupancy on several tRNA genes. Interestingly, the effect of YPD→YPGly transition on the occupancy of TFIIIC was more prominent for intron-containing tRNA genes for which longer distance between A- and B-boxes was noted (Figure 1A). Therefore, one hypothesis is that this longer distance may be a factor that facilitates TFIIIC binding to tRNA genes during repression. Pronounced repression of intron-containing genes by Maf1 could be in part assisted by TFIIIC binding.

With the knowledge that Maf1 is involved in coupling carbon metabolism to Pol III transcription (31), we monitored the effects of *maf1Δ* on occupancy of TFIIIC and Pol III on tRNA genes under various physiological conditions. In YPD-grown cells, Maf1 was inactive, and as expected, no significant difference in tDNA occupancy by Pol III machinery was observed between *maf1Δ* and control strain. Notably, inactivation of Maf1 resulted in a decrease in TFIIIC and increase in Pol III occupancy under all other growth conditions tested (YPGly, YPGly and YPGly+glucose). In summary, TFIIIC and Pol III occupancy are dependent on Maf1 in opposite fashion (Figure 5, upper panel).

Maf1 appears to interact directly with Pol III and prevent Pol III recruitment to tRNA genes during repression (10). Therefore, an increased Pol III occupancy on tRNA genes in the absence of Maf1 appears reasonable. Hence, an opposite effect of Maf1 inactivation on TFIIIC occupancy is probably indirect and a result of full competition between Pol III and TFIIIC, both during active transcription and under repressive conditions. Although no data on Maf1 interaction with TFIIIC has been reported, the scenario in which Maf1 promotes TFIIIC-mediated repression cannot be excluded. Our previous estimation indicated that only a small portion of Maf1 is associated with Pol III (12), suggesting that other Maf1 targets may exist.

Whereas Pol III displaces TFIIIC during active transcription, TFIIIC replaces Pol III when conditions are unfavorable for transcription to proceed. An important question is whether TFIIIC represents only a transient barrier for Pol III or acts as an active repressor. All subunits of TFIIIC are essential and the relatively sparse data indicate that their expression must be tightly regulated (39). Moreover, several links between metabolism and signaling cascades have recently been established. In particular, the τ55 subunit of TFIIIC is an active phosphatase (40), TFIIIC is in contact with TOR (41), and current data indicate a direct control of TFIIIC by PKA (Figure 3A and B; Supplementary Figure S3). Recruitment of TFIIIC may be also related to its function in chromatin organization (42–44) and co-localization with condensins (45). Altogether, regulation of TFIIIC function/activity is not well-known, but previous and current data do not exclude its active functioning under repressive conditions.

Although the most important function of TFIIIC in initiation of transcription on tRNA genes is the recruitment of TFIIIB, the molecular mechanisms of this process are not fully understood. Based on a yeast two-hybrid system and genetic analyses, recruitment of both Brf1 and Bdp1 is directed by the TPR repeat domains of the τ131 subunit of TFIIIC (7,36,37,46). Currently proposed model of TFIIIC architecture (16) allows for mapping and analysis of TFIIIC mutations that have been previously described and design of polypeptides for biochemical pull-down experiments aimed at studying τ131 interactions with the τ138 subunit of τB and subunits of TFIIIB, Brf1 and Bdp1. The model assumes τ131 N-terminal domain binding of Brf1 as an initial recruitment step, followed by TBP recruitment via Brf1 and the τ60 subunit of τB, and finally, binding of Bdp1 to τ131. Competition between Bdp1 and τ138 τB subunits to bind the same domain of τ131 suggests that recruitment of Bdp1 induces a conformational change, leading to displacement of the τB module and consequently, dissociation of TFIIIC from the gene (16).

Here, we analyzed how Pol III induction upon YPGly→YPGly+glucose transition would be correlated with TFIIIB–TFIIIC interaction and TFIIIB recruitment to tDNA. To our surprise, the increased recruitment of Brf1 and Bdp1 to tDNA genes was correlated with their release from TFIIIC (Figure 4). Noteworthy, the association of Bdp1 and Brf1 with τ131 is strong in YPGly-grown cells (Figure 4A) suggesting that these TFIIIB subunits form a stable complex with TFIIIC under repressive conditions. The process of Brf1 and Bdp1 assembly with τ131 is therefore distinct from TFIIIB recruitment to tDNA. We hypothesize that Brf1 and Bdp1 are deposited in the complex with TFIIIC until transcription is induced by environmental signal. Then, Brf1 and Bdp1 must be transferred to tDNA. Alternatively, Brf1 and Bdp1 may be transferred to tDNA separately, in coordination with the recruitment of TBP via the τ60 subunit. Interaction of τ60 with TBP and a direct role of τB in TFIIIB recruitment were described before (47,48). In promoters consisting of just a TATA box, binding of TFIIIB to the DNA involves recognition of the TATA box by its TBP subunit (49). Our current view of the TFIIIB–DNA complex formation was created by *in vitro* studies and structure analyses in which TATA box-containing templates were applied (50,51). Further studies are required to determine how the recruitment of Brf1, TBP and Bdp1 subunits leads to the formation of a TFIIIB complex with TATA-less promoters in tRNA genes of *S. cerevisiae*.

Our results are consistent with a previous immunoprecipitation study that detected an increase in the interaction between Bdp1 and τ95, another subunit of the τA module, upon starvation and a decrease when glucose was added (13), although no effect of these growth conditions on Bdp1 recruitment to DNA was identified (13). Moreover, we did not observe a significant change in the τ131–τ138 interaction upon Pol III activation by YPGly→YPGly+glucose transition. Furthermore, our results suggest a regulatory mechanism for this interaction based on the phosphorylation of τ138. Inactivation of potential sites of phosphorylation by PKA in the τ138 subunit strengthened the intramolecular interactions within the TFIIIC complex (Figure 3E). Possibly, the competition between τ138 and Bdp1 for τ131 binding does not impair τA–τB interaction but rather induces conformational rearrangements necessary to deposit TFIIIB onto DNA. This hypothesis is complementary to the model proposed by Male *et al.* (16).

Our observations suggest the following speculative model for control of Pol III transcription by TFIIIC (Figure 5, lower panel). In its natural environment, yeast cells are usually maintained in the repressed state. During repression, TFIIIC is bound to A- and B-boxes in tRNA genes. Two subunits of TFIIIB, Brf1 and Bdp1, are assembled and bound to the τ131 subunit of TFIIIC. Pol III is inactive when complexed with Maf1. Induction of transcription by environmental signals leads to conformational changes in TFIIIC, which leads to stepwise dissociation of TFIIIC from tDNA. The conformational change in TFIIIC also involves dissociation of Brf1 and Bdp1 from τ131 and increases their association with tDNA, possibly with the contribution of TBP, pre-bound to the τ60 subunit. At the same time, Maf1 is phosphorylated and dissociates from the Pol III complex, which becomes active. Then TFIIIB recruits Pol III to the transcription start site (which is no longer covered by TFIIIC), forming the initial transcription complex. Subsequent conformational changes in Pol III machinery lead to formation of an elongation complex and displacement of TFIIIC from tDNA by the transcribing polymerase. In summary, our present work reveals several new aspects of the mechanism of TFIIIB assembly and control of tRNA gene transcription by its general transcription factor, TFIIIC.

SUPPLEMENTARY DATA

Supplementary Data are available at NAR Online.

ACKNOWLEDGEMENTS

We thank Michał Kępka for the construction of τ138–*3StA* mutant. Ewa Leśniewska, Damian Graczyk and Andrzej Dziembowski for critical reading of the manuscript and Szymon Świeżewski for stimulating discussions.

FUNDING

National Science Centre [UMO-2012/04/A/NZ1/00052]; Foundation for Polish Science [MISTRZ 7/2014]. Funding for open access charge: Department of Genetics, Polish Academy of Sciences.
Conflict of interest statement. None declared.

REFERENCES

1. Vorländer,M.K., Khatter,H., Wetzel,R., Hagen,W.J.H. and Müller,C.W. (2018) Molecular mechanism of promoter opening by RNA polymerase III. *Nature*, **553**, 295–300.
2. Abascal-Palacios,G., Ramsay,E.P., Beuron,F., Morris,E. and Vannini,A. (2018) Structural basis of RNA polymerase III transcription initiation. *Nature*, **553**, 301–306.
3. Sentenac,A. and Riva,M. (2013) Odd RNA polymerases or the A(B)C of eukaryotic transcription. *Biochim. Biophys. Acta*, **1829**, 251–257.
4. Geiduschek,E.P. and Kassavetis,G.A. (2001) The RNA polymerase III transcription apparatus. *J. Mol. Biol.*, **310**, 1–26.

5. Schramm,L. and Hernandez,N. (2002) Recruitment of RNA polymerase III to its target promoters. *Genes Dev.*, **16**, 2593–2620.
6. Dieci,G., Fiorino,G., Castelnuovo,M., Teichmann,M. and Pagano,A. (2007) The expanding RNA polymerase III transcriptome. *Trends Genet.*, **23**, 614–622.
7. Ramsay,E.P. and Vannini,A. (2018) Structural rearrangements of the RNA polymerase III machinery during tRNA transcription initiation. *Biochim. Biophys. Acta*, **1861**, 285–294.
8. Acker,J., Conesa,C. and Lefebvre,O. (2013) Yeast RNA polymerase III transcription factors and effectors. *Biochim. Biophys. Acta*, **1829**, 283–295.
9. Nagarajavel,V., Iben,J.R., Howard,B.H., Maraia,R.J. and Clark,D.J. (2013) Global 'bootprinting' reveals the elastic architecture of the yeast TFIIIB-TFIIIC transcription complex in vivo. *Nucleic Acids Res.*, **41**, 8135–8143.
10. Vannini,A., Ringel,R., Kusser,A.G., Berninghausen,O., Kassavetis,G.A. and Cramer,P. (2010) Molecular basis of RNA polymerase III transcription repression by Maf1. *Cell*, **143**, 59–70.
11. Pluta,K., Lefebvre,O., Martin,N.C., Smagowicz,W.J., Stanford,D.R., Ellis,S.R., Hopper,A.K., Sentenac,A. and Boguta,M. (2001) Maf1p, a negative effector of RNA Polymerase III in saccharomyces cerevisiae. *Mol. Cell. Biol.*, **21**, 5031–5040.
12. Oficjalska-Pham,D., Harismendy,O., Smagowicz,W.J., Gonzalez de Peredo,A., Boguta,M., Sentenac,A. and Lefebvre,O. (2006) General repression of RNA polymerase III transcription is triggered by protein phosphatase type 2A-mediated dephosphorylation of Maf1. *Mol. Cell*, **22**, 623–632.
13. Roberts,D.N., Wilson,B., Huff,J.T., Stewart,A.J. and Cairns,B.R. (2006) Dephosphorylation and Genome-Wide association of Maf1 with Pol III-Transcribed genes during repression. *Mol. Cell*, **22**, 633–644.
14. Desai,N., Lee,J., Upadhya,R., Chu,Y., Moir,R.D. and Willis,I.M. (2005) Two steps in Maf1-dependent repression of transcription by RNA polymerase III. *J. Biol. Chem.*, **280**, 6455–6462.
15. Dumay-Odelot,H., Marck,C., Durrieu-Gaillard,S., Lefebvre,O., Jourdain,S., Prochazkova,M., Pflieger,A. and Teichmann,M. (2007) Identification, molecular cloning, and characterization of the sixth subunit of human transcription factor TFIIIC. *J. Biol. Chem.*, **282**, 17179–17189.
16. Male,G., von Appen,A., Glatt,S., Taylor,N.M.I., Cristovao,M., Groetsch,H., Beck,M. and Müller,C.W. (2015) Architecture of TFIIIC and its role in RNA polymerase III pre-initiation complex assembly. *Nat. Commun.*, **6**, 7387–7395.
17. Ruet,A., Camier,S., Smagowicz,W., Sentenac,A. and Fromageot,P. (1984) Isolation of a class C transcription factor which forms a stable complex with tRNA genes. *EMBO J.*, **3**, 343–350.
18. Roberts,D.N., Stewart,A.J., Huff,J.T. and Cairns,B.R. (2003) The RNA polymerase III transcriptome revealed by genome-wide localization and activity-occupancy relationships. *Proc. Natl. Acad. Sci. U.S.A.*, **100**, 14695–14700.
19. Moqtaderi,Z. and Struhl,K. (2004) Genome-wide occupancy profile of the RNA polymerase III machinery in Saccharomyces cerevisiae reveals loci with incomplete transcription complexes. *Mol. Cell. Biol.*, **24**, 4118–4127.
20. Soragni,E. and Kassavetis,G.A. (2008) Absolute gene occupancies by RNA polymerase III, TFIIIB, and TFIIIC in Saccharomyces cerevisiae. *J. Biol. Chem.*, **283**, 26568–26576.
21. Turowski,T.W., Leśniewska,E., Delan-Forino,C., Sayou,C., Boguta,M. and Tollervey,D. (2016) Global analysis of transcriptionally engaged yeast RNA polymerase III reveals extended tRNA transcripts. *Genome Res.*, **26**, 933–944.
22. Bodenmiller,B., Campbell,D., Gerrits,B., Lam,H., Jovanovic,M., Picotti,P., Schlapbach,R. and Aebersold,R. (2008) PhosphoPep–a database of protein phosphorylation sites in model organisms. *Nat. Biotechnol.*, **26**, 1339–1340.
23. Gao,X., Jin,C., Ren,J., Yao,X. and Xue,Y. (2008) Proteome-wide prediction of PKA phosphorylation sites in eukaryotic kingdom. *Genomics*, **92**, 457–463.
24. Sadowski,I., Breitkreutz,B.-J., Stark,C., Su,T.-C., Dahabieh,M., Raithatha,S., Bernhard,W., Oughtred,R., Dolinski,K., Barreto,K. *et al.* (2013) The PhosphoGRID Saccharomyces cerevisiae protein phosphorylation site database: version 2.0 update. *Database*, **2013**, bat026.
25. Conesa,C., Swanson,R.N., Schultz,P., Oudet,P. and Sentenac,A. (1993) On the subunit composition, stoichiometry, and phosphorylation of the yeast transcription factor TFIIIC/tau. *J. Biol. Chem.*, **268**, 18047–18052.
26. Ptacek,J., Devgan,G., Michaud,G., Zhu,H., Zhu,X., Fasolo,J., Guo,H., Jona,G., Breitkreutz,A., Sopko,R. *et al.* (2005) Global analysis of protein phosphorylation in yeast. *Nature*, **438**, 679–684.
27. Graczyk,D., Debski,J., Muszyńska,G., Bretner,M., Lefebvre,O. and Boguta,M. (2011) Casein kinase II-mediated phosphorylation of general repressor Maf1 triggers RNA polymerase III activation. *Proc. Natl. Acad. Sci. U.S.A.*, **108**, 4926–4931.
28. Ren,B., Robert,F., Wyrick,J.J., Aparicio,O., Jennings,E.G., Simon,I., Zeitlinger,J., Schreiber,J., Hannett,N., Kanin,E. *et al.* (2000) Genome-wide location and function of DNA binding proteins. *Science*, **290**, 2306–2309.
29. Foretek,D., Wu,J., Hopper,A.K. and Boguta,M. (2016) Control of Saccharomyces cerevisiae pre-tRNA processing by environmental conditions. *RNA*, **22**, 339–349.
30. Cieśla,M., Makała,E., Płonka,M., Bazan,R., Gewartowski,K., Dziembowski,A. and Boguta,M. (2015) Rbs1, a new protein implicated in RNA polymerase III biogenesis in yeast Saccharomyces cerevisiae. *Mol. Cell. Biol.*, **35**, 1169–1181.
31. Cieśla,M., Towpik,J., Graczyk,D., Oficjalska-Pham,D., Harismendy,O., Suleau,A., Balicki,K., Conesa,C., Lefebvre,O. and Boguta,M. (2007) Maf1 is involved in coupling carbon metabolism to RNA polymerase III transcription. *Mol. Cell. Biol.*, **27**, 7693–7702.
32. Karkusiewicz,I., Turowski,T.W., Graczyk,D., Towpik,J., Dhungel,N., Hopper,A.K. and Boguta,M. (2011) Maf1 protein, repressor of RNA polymerase III, indirectly affects tRNA processing. *J. Biol. Chem.*, **286**, 39478–39488.
33. Conrad,M., Schothorst,J., Kankipati,H.N., Van Zeebroeck,G., Rubio-Texeira,M. and Thevelein,J.M. (2014) Nutrient sensing and signaling in the yeast Saccharomyces cerevisiae. *FEMS Microbiol. Rev.*, **38**, 254–299.
34. Schepers,W., Van Zeebroeck,G., Pinkse,M., Verhaert,P. and Thevelein,J.M. (2012) In vivo phosphorylation of Ser21 and Ser83 during nutrient-induced activation of the yeast protein kinase A (PKA) target trehalase. *J. Biol. Chem.*, **287**, 44130–44142.
35. Moir,R.D., Lee,J., Haeusler,R.A., Desai,N., Engelke,D.R. and Willis,I.M. (2006) Protein kinase A regulates RNA polymerase III transcription through the nuclear localization of Maf1. *Proc. Natl. Acad. Sci. U.S.A.*, **103**, 15044–15049.
36. Dumay-Odelot,H., Acker,J., Arrebola,R., Sentenac,A. and Marck,C. (2002) Multiple roles of the tau131 subunit of yeast transcription factor IIIC (TFIIIC) in TFIIIB assembly. *Mol. Cell. Biol.*, **22**, 298–308.
37. Liao,Y., Willis,I.M. and Moir,R.D. (2003) The Brf1 and Bdp1 subunits of transcription factor TFIIIB bind to overlapping sites in the tetratricopeptide repeats of Tfc4. *J. Biol. Chem.*, **278**, 44467–44474.
38. Harismendy,O., Gendrel,C.-G., Soularue,P., Gidrol,X., Sentenac,A., Werner,M. and Lefebvre,O. (2003) Genome-wide location of yeast RNA polymerase III transcription machinery. *EMBO J.*, **22**, 4738–4747.
39. Kleinschmidt,R.A., LeBlanc,K.E. and Donze,D. (2011) Autoregulation of an RNA polymerase II promoter by the RNA polymerase III transcription factor III C (TF(III)C) complex. *Proc. Natl. Acad. Sci. U.S.A.*, **108**, 8385–8389.
40. Taylor,N.M.I., Glatt,S., Hennrich,M.L., von Scheven,G., Grötsch,H., Fernández-Tornero,C., Rybin,V., Gavin,A.-C., Kolb,P. and Müller,C.W. (2013) Structural and functional characterization of a phosphatase domain within yeast general transcription factor IIIC. *J. Biol. Chem.*, **288**, 15110–15120.
41. Kantidakis,T., Ramsbottom,B.A., Birch,J.L., Dowding,S.N. and White,R.J. (2010) mTOR associates with TFIIIC, is found at tRNA and 5S rRNA genes, and targets their repressor Maf1. *Proc. Natl. Acad. Sci. U.S.A.*, **107**, 11823–11828.
42. Simms,T.A., Dugas,S.L., Gremillion,J.C., Ibos,M.E., Dandurand,M.N., Toliver,T.T., Edwards,D.J. and Donze,D. (2008) TFIIIC binding sites function as both heterochromatin barriers and chromatin insulators in Saccharomyces cerevisiae. *Eukaryot. Cell*, **7**, 2078–2086.

43. Donze,D. (2012) Extra-transcriptional functions of RNA Polymerase III complexes: TFIIIC as a potential global chromatin bookmark. *Gene*, **493**, 169–175.
44. Mertens,C. and Roeder,R.G. (2008) Different functional modes of p300 in activation of RNA polymerase III transcription from chromatin templates. *Mol. Cell. Biol.*, **28**, 5764–5776.
45. D'Ambrosio,C., Schmidt,C.K., Katou,Y., Kelly,G., Itoh,T., Shirahige,K. and Uhlmann,F. (2008) Identification of cis-acting sites for condensin loading onto budding yeast chromosomes. *Genes Dev.*, **22**, 2215–2227.
46. Moir,R.D., Sethy-Coraci,I., Puglia,K., Librizzi,M.D. and Willis,I.M. (1997) A tetratricopeptide repeat mutation in yeast transcription factor IIIC131 (TFIIIC131) facilitates recruitment of TFIIB-related factor TFIIIB70. *Mol. Cell. Biol.*, **17**, 7119–7125.
47. Deprez,E., Arrebola,R., Conesa,C. and Sentenac,A. (1999) A subunit of yeast TFIIIC participates in the recruitment of TATA-binding protein. *Mol. Cell. Biol.*, **19**, 8042–8051.
48. Mylona,A., Fernández-Tornero,C., Legrand,P., Haupt,M., Sentenac,A., Acker,J. and Müller,C.W. (2006) Structure of the tau60/Delta tau91 subcomplex of yeast transcription factor IIIC: insights into preinitiation complex assembly. *Mol. Cell*, **24**, 221–232.
49. Strubin,M. and Struhl,K. (1992) Yeast and human TFIID with altered DNA-binding specificity for TATA elements. *Cell*, **68**, 721–730.
50. Whitehall,S.K., Kassavetis,G.A. and Geiduschek,E.P. (1995) The symmetry of the yeast U6 RNA gene's TATA box and the orientation of the TATA-binding protein in yeast TFIIIB. *Genes Dev.*, **9**, 2974–2985.
51. Cloutier,T.E., Librizzi,M.D., Mollah,A.K., Brenowitz,M. and Willis,I.M. (2001) Kinetic trapping of DNA by transcription factor IIIB. *Proc. Natl. Acad. Sci. U.S.A.*, **98**, 9581–9586.